



This is a repository copy of *Microscopic investigation of subsurface initiated damage of wind turbine gearbox bearings*.

White Rose Research Online URL for this paper:
<http://eprints.whiterose.ac.uk/139867/>

Version: Published Version

Proceedings Paper:

Al-Bedhany, J.H. and Long, H. orcid.org/0000-0003-1673-1193 (2018) Microscopic investigation of subsurface initiated damage of wind turbine gearbox bearings. In: *Journal of Physics: Conference Series. Modern Practice in Stress and Vibration Analysis (MPSVA) 2018*, 02-04 Jul 2018, Cambridge, UK. IOP Publishing .

<https://doi.org/10.1088/1742-6596/1106/1/012029>

Reuse

This article is distributed under the terms of the Creative Commons Attribution (CC BY) licence. This licence allows you to distribute, remix, tweak, and build upon the work, even commercially, as long as you credit the authors for the original work. More information and the full terms of the licence here:
<https://creativecommons.org/licenses/>

Takedown

If you consider content in White Rose Research Online to be in breach of UK law, please notify us by emailing eprints@whiterose.ac.uk including the URL of the record and the reason for the withdrawal request.



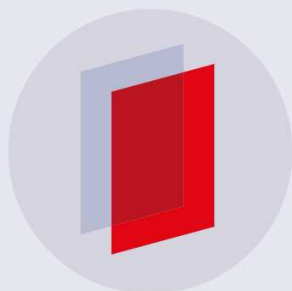
eprints@whiterose.ac.uk
<https://eprints.whiterose.ac.uk/>

PAPER • OPEN ACCESS

Microscopic investigation of subsurface initiated damage of wind turbine gearbox bearings

To cite this article: Jasim H Al-Bedhany and Hui Long 2018 *J. Phys.: Conf. Ser.* **1106** 012029

View the [article online](#) for updates and enhancements.



IOP | ebooks™

Bringing you innovative digital publishing with leading voices to create your essential collection of books in STEM research.

Start exploring the collection - download the first chapter of every title for free.

Microscopic investigation of subsurface initiated damage of wind turbine gearbox bearings

Jasim H AL-Bedhany and Hui Long*

Department of Mechanical Engineering, The University of Sheffield, Sheffield, UK.

* h.long@sheffield.ac.uk

Abstract. Wind turbine gearbox bearings experience premature failures by White Structure Flaking (WSF), often occurs much earlier than their designed life of 20 to 25 years. This results in increased operational and maintenance costs due to unplanned maintenance and early replacement. The main causes and damage initiation mechanism of this premature failure are not fully understood; despite extensive research and investigation in recent years. In this paper, two planetary bearings from a failed gearbox of a multi-megawatt wind turbine are destructively investigated to characterize the subsurface microstructural damage and to understand damage initiation mechanism leading to surface WSF. The results show that the non-metallic inclusions are not the only initiator of subsurface damage. The microcracks are also initiated in the subsurface to form macrocracks which then propagate or connect to other macrocracks to reach the rolling contact surface causing WSF. The characterization of different forms of subsurface microstructural damage shows a close correlation of the maximum shear stress with the damage initiation. Butterfly wings are found to initiate from the compound type of non-metallic inclusions with low aspect ratio and to be associated with inclusion internal cracking in a direction approximately parallel to the axis of the maximum wing length.

1. Introduction

The designed life of wind turbines (WTs) is 20 to 25 years however the premature failure of wind turbine gearbox (WTG) bearings by White Structure Flaking (WSF) has often been reported[1]. This failure is associated with microstructural alterations beneath the rolling contact surfaces of bearing raceways and rolling elements[1][2][3]. Despite extensive research effort investigating the bearing premature failure by WSF, the main causes and damage initiation and propagation mechanisms are still a scientific and debateable subject[4][5]. Microscopic investigation of samples obtained from failed bearings of field operating WTGs provides an insight into the microstructural alterations and various forms of damage occurred. Energy Dispersive X-ray Analysis (EDX) technique is commonly used to specify the chemical compositions of the bearing materials and other microstructural defects such as non-metallic inclusions[6].

Different forms of microstructural damage, especially butterfly wings, were investigated by a considerable number of studies[7][8][9]. The results found that the formation of microstructural alterations occurred at a specific depth range from the rolling contact surface. The butterfly wings approximately looked like shear stress distributions induced by contact pressure, which led to suggestions that the shear stress had an important effect on the initiation of this damage[10][11][12]. Non-metallic inclusions and material cleanliness had an important effect on damage initiation[13][14][15][16]. The inclusion type, size and distribution were the main parameters effecting



the damage initiation[17][18]. Destructive investigation by sectioning the failed region of WTG bearings provided a two-dimensional view of investigated plane while serial sectioning technique allowed approximately a three-dimensional observation of cracking network[19].

In this study, a destructive investigation of two failed WTG planetary bearings is conducted to study the severely damaged regions of the bearing raceways by microscopic examination and to characterize different forms of damage such as butterfly wings, microcracks and damaged inclusions. The results show that the subsurface microcracks are another initiator of WSF initiation, in addition to the WSF resulted from non-metallic inclusions. Subsurface maximum shear stress has an important effect on the initiation of different forms of damage such as butterfly wings, inclusions with internal cracking and inclusions separations at inclusion-steel matrix boundaries.

2. Microscopic investigation

In this study, the severely damaged regions of two planetary bearings are destructively investigated. The samples for microscopic investigation are cut and examined in both axial and circumferential directions of the bearing raceway, as illustrated in figure 1. Samples are mounted using conductive resins to show the investigated surfaces. By using this cutting procedure, the entire axial plane located in the centreline of the severely damaged zone as well as six equally spaced circumferential sections of the raceway can be microscopically investigated. Samples are grinded, polished then etched with 2% Nital (2% Nitric acid and 98% ethanol). Optical microscope and Scanning Electron Microscope (SEM) are used in parallel with EDX technique to investigate the microstructure alterations and different forms of damage. Damage forms such as inclusion-initiated cracks and butterfly wings are characterised according to their damage features defined by dimensions, depth beneath the rolling contact surface, inclination angle relative to the rolling surface and inclusion Aspect Ratio (AR). The subsurface damage initiation is analysed by correlating the damage features with possible loading conditions experienced by the bearings during their operation. Subsurface stress distributions beneath the contact surface and the stress variation due to various loading levels are determined using Hertzian contact theory. Stresses distributions under the effect of surface traction are also calculated to analyse its expected role on damage initiation.

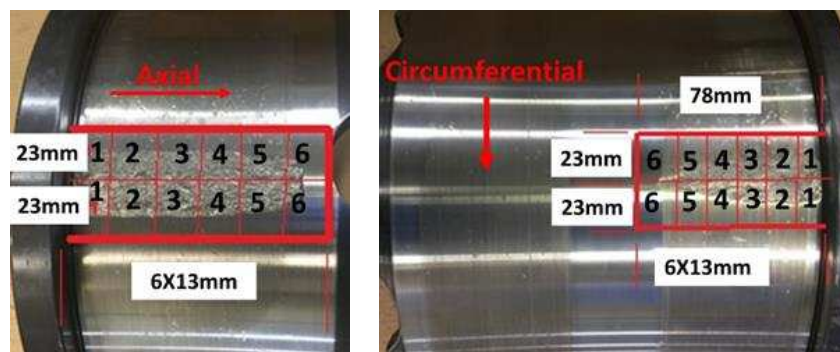


Figure 1. Investigated failed bearings and sample locations (upwind and downwind bearing raceways).

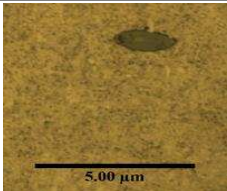
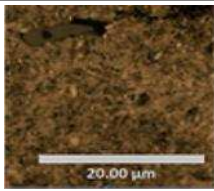
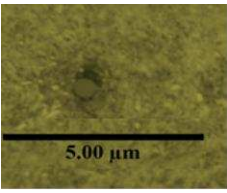

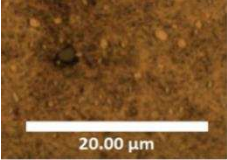

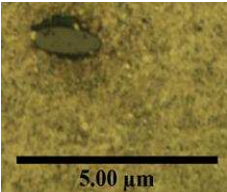
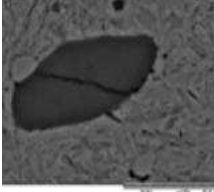
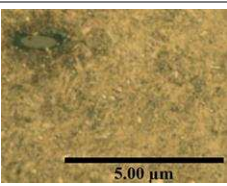
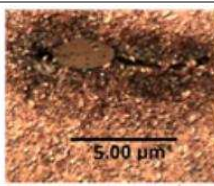
3. Results and discussions

In this study, 149 damaged inclusions are found, of which 55 inclusions (37%) are in the two axial sectioned samples and 94 inclusions (63%) are in the two circumferential-sectioned samples. These samples are chosen from the middle of axial and circumferential-sectioned samples, i.e. sample 3 and 4 as shown in Figure 1. The depths of these samples investigated are within 1 mm beneath the rolling contact surface, since the effect of maximum contact stresses do not expect to go beyond this depth[1][12].

Damaged inclusions either have separation damage, i.e. inclusions deboned at their boundaries from steel matrix, cracking damage or mixed damage of separation and cracking. [table 1](#) illustrates these damage forms. Four different types of inclusion damage by separation are identified: upper separation, lower separation, upper and lower separation, and side separations.

Most distinctive microstructural alterations found are butterfly wings. Therefore, the investigation and analysis of this paper focus on this damage form. Butterfly wings are classified into single and double winged butterflies, and single winged butterflies are further classified into upper and lower single winged respectively. The upper winged butterflies have the butterfly wing above the damage initiating inclusion i.e. from the inclusion towards the rolling contact surface. The lower winged butterflies crack away from the rolling contact surface. The characterization parameters, including wing length, inclusion angle and depth of 49 butterflies, are analysed.

Table 1. Different forms of microstructural damage initiated by inclusions.

Separation at inclusion		Cracking at inclusion	
Damage type	Examples	Damage type	Examples
No separation		Upper cracking	
Upper separation		Lower cracking	
Lower separation		Upper and lower cracking	
Upper and lower separation		Cracked inclusion	
Side separations		Mixed types of cracking	

3.1. Characterization of damage initiating inclusions

Subsurface stress distributions beneath the contact surface are calculated using Hertzian contact theory by applying compression and traction loading according to the designed stress level specified by the international standards[20][21]. [figure 2](#) shows the distributions of the maximum shear stress when under compression only and under combined compression and traction respectively. Increasing the compressive loading moves the maximum shear stress zone further away from the contact surface. Introducing surface traction into compression moves the maximum shear stress zone closer towards

the contact surface. The maximum shear stress zone will be compared with the locations where various forms of damage are found in the following sections.

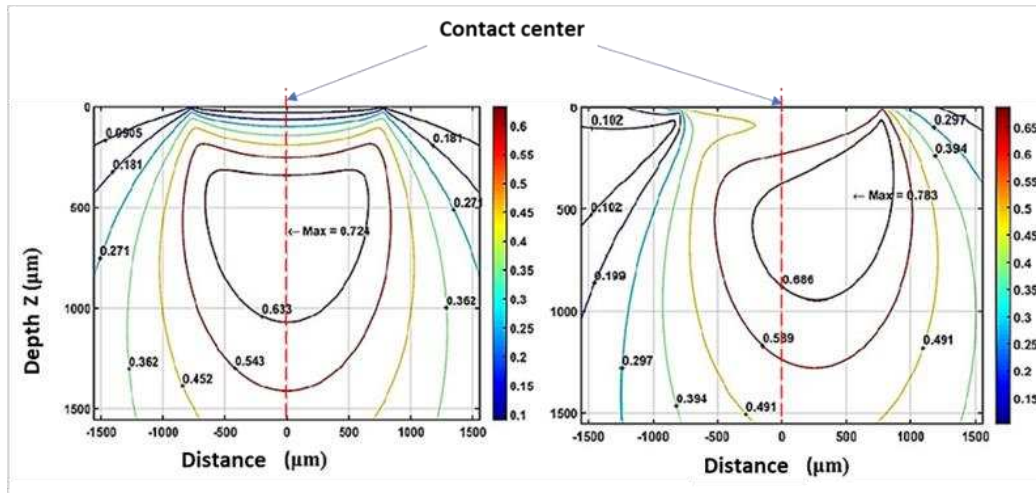


Figure 2. Distributions of maximum shear stress (in GPa), (left) under compression loading 1.8 GPa and (right) under combined compression loading 1.8 GPa and 0.2% traction.

Different forms of inclusion related damage are found in subsurface of the bearing rolling contact, including: inclusions separated from the matrix, cracks extended from inclusion into the matrix and butterfly wings. Percentages of different types of damaged inclusions with their depths are presented in figures 3 and 4. All separated inclusions are found to be located approximately within the depth of the maximum shear stress zone in the subsurface of the contact. For inclusions with separation in the centre of the upper side of the inclusion boundary, the damage may be due to shear stresses with surface traction, since the traction effect brings the maximum shear stress zone closer to the contact surface. The numbers of inclusions with separation at the lower side of the inclusion increase with the depth. By comparing the depths of damaged inclusions by separation in figure 3(a) with the depth of the maximum shear stress shown in figure 2, it is clear their depths are closely correlated.

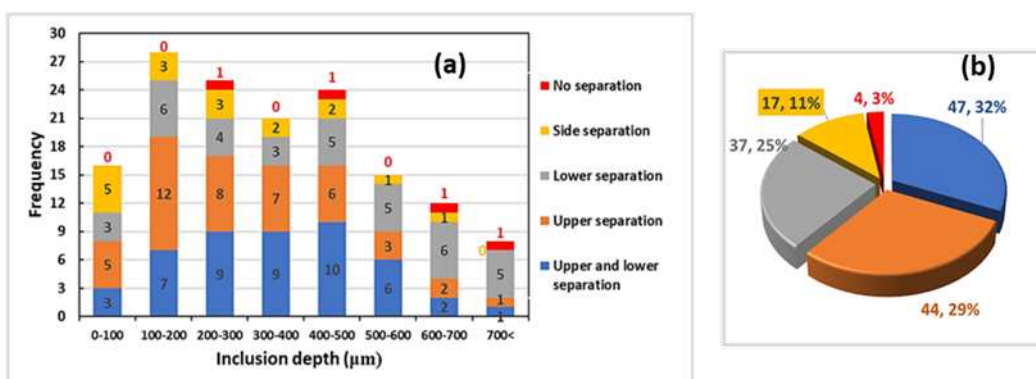


Figure 3. Damaged inclusions by separation: a) in relation to subsurface depth; b) numbers and percentages of separated inclusions.

Inclusions with separation are the most dominant damage form however damaged inclusions by cracking are also observed. The cracks appear in different forms: in the tip of the upper side of the inclusion (towards the rolling contact surface), in the tip of the lower side of the inclusion, internal cracking of the inclusion itself, or combined cracking of these different forms. Inclusions associated with cracks are approximately located within the depth of maximum shear stress in the subsurface of

the contact as shown in [figure 4](#). The characterization of damaged inclusions supports the previous suggestion that the inclusion-initiated damage in subsurface may be resulted from effects of shear stresses and the cracking appears along the maximum shear stress plane.

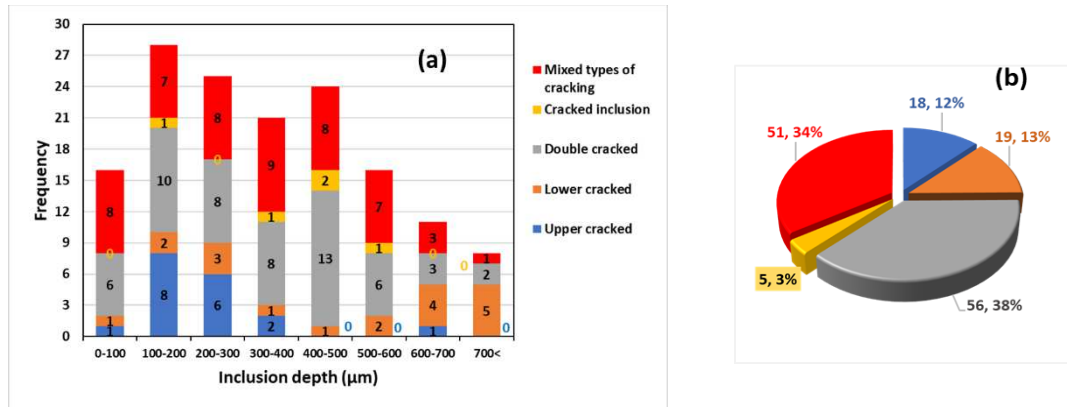


Figure 4. Damaged inclusions by cracking: a) in relation to subsurface depth; b) numbers and percentages of cracked inclusions.

3.2. Butterfly wings

The depth distribution of the 49 observed butterfly wings is shown in [figure 5\(a\)](#). All butterflies are in the circumferential-sectioned samples, approximately located at the depth of the maximum shear stress. Number of butterflies observed increases with increasing depth, however no butterfly is found in depth greater than 700 μm. Only one small butterfly wing is found parallel to the contact surface. Considerable butterfly wings have an inclined angle to the rolling contact surface at 25° or 40° respectively, counted as 29% and 21% of all butterflies, as shown in [figure 5\(b\)](#). [figure 5\(c\)](#) presents the distribution of butterfly wings according to the lengths of their wings. Because the investigated samples are cut from the severely damaged region of the bearing raceways where some parts of the contact surface are removed by severe spalling therefore no butterflies are found in shallow depths of the rolling contact surface.

Around 71% of the butterflies found have double wings while 57% of the remaining butterflies (29% of all butterflies found) have single wing at the upper side of the initiation inclusion and the rest butterflies have single wing at the lower side. Single winged butterflies have shorter lengths when compared with the double winged butterflies. This leads to a hypothesis that butterfly wings may have initiated as a single wing first and the other wing appeared later, then they propagated together to grow into longer wings. There is no evidence to support whether the upper or the lower wing has initiated first however the point of wing initiation may depend on the location of the damage initiating inclusion in relation to the location of maximum shear stress. These observations support the suggestion that the maximum shear stress is an influence factor on the initiation of butterfly microstructure damage [22]. It is observed that cracks associated with butterfly wings are probably not a part of macrocrack network that linked to rolling contact surfaces because they disappear after regrinding the sample surfaces where the butterfly wings are observed. However, the butterfly cracks may not play an important role on subsurface damage propagation. All forms of damage are probably produced due to the shear stress levels have exceeded a critical limit of the bearing material.

There is no clear correlation between the depths of damaged inclusions with the occurrence of butterflies with upper or lower wing. [figure 6\(a\)](#) shows two inclusions located approximately at the same depth (~320 μm); however, one inclusion has an upper single wing while another has a lower single wing. [figure 6\(b\)](#) shows two inclusions with butterfly wings, the inclusion with an upper wing is located at depth of ~250 μm; however, the inclusion with a lower wing is located deeper at ~148 μm.

Damaged inclusions, microcracks, and butterfly wings are located deeper than the region of the maximum shear stress calculated, which indicates that the contact surfaces may have been subjected to

much higher loading levels than designed stress level specified by the international standards, possibly exceeded the yield strength of the bearing material. To confirm this, hardness of the bearing raceway contact surface inside and outside the loading zones are measured at 25 points then averaged. The surface hardness outside and inside the loading zones are 746 HV and 788 HV respectively and this indicates that the surface inside the loading zone has been hardened due to overloading.

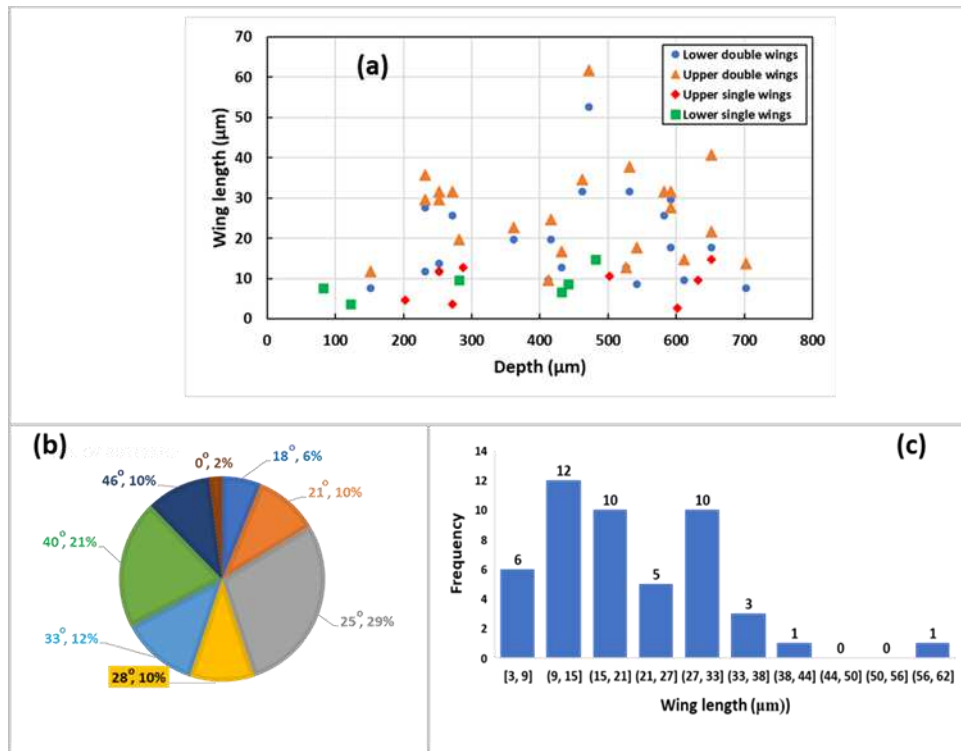


Figure 5. Butterflies: a) wing lengths in relation to subsurface depth; b) wing angles and percentages c) occurrences in relation to wing length.

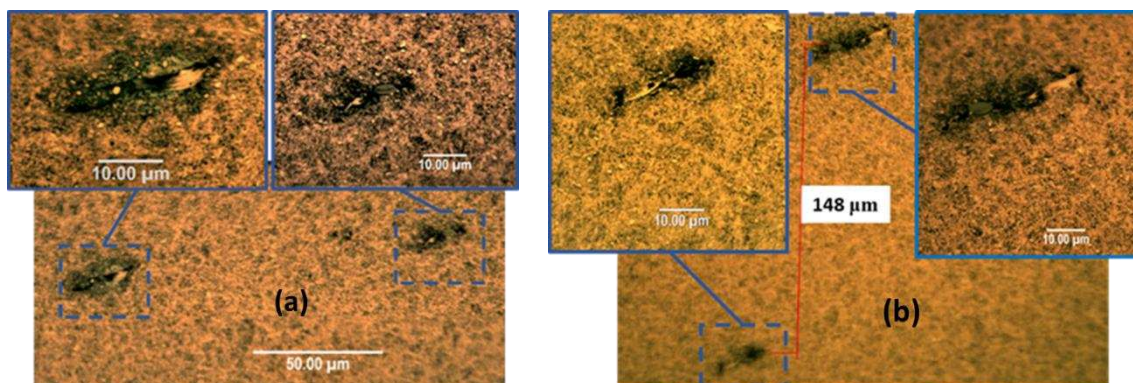


Figure 6. Depths of butterflies a) two butterflies with upper / lower wing located at the same depth; b) two butterflies with upper / lower wings located at different depths.

One of the largest butterflies found in this study is shown in figure 7(a). It is located at the end region of the severely spalling area away from rim of the downwind bearing (sample No.6 in figure 1). This butterfly has a depth of ~470 µm beneath the rolling contact surface, within the maximum shear stress zone as shown in figure 2. The inclusion in the centre of the butterfly wings shown in figure 7(b)

has a darker colour compared to that of MnS inclusions which have light grey colour[13]. Energy Dispersive X-ray (EDX) analysis is used to confirm the inclusion's chemical compositions, as shown in figure 7(c). The analysis shows that it is a compound inclusion of MnS, aluminium oxide and silica in addition to other chemical compositions. Thus it is the inclusion type D_{Dup} according to the International Standard ISO-4967:2013[13]. Aspect Ratio (AR) is defined as the ratio of inclusion lengths along the major to minor axes and it is used to evaluate the inclusion shape. It is found that the majority of the butterflies are initiated at inclusions having low aspect ratio of around 2:1. It is also observed that the butterflies are likely associated with inclusions with internal cracks in a direction approximately parallel to the direction of maximum length of the butterfly wing.

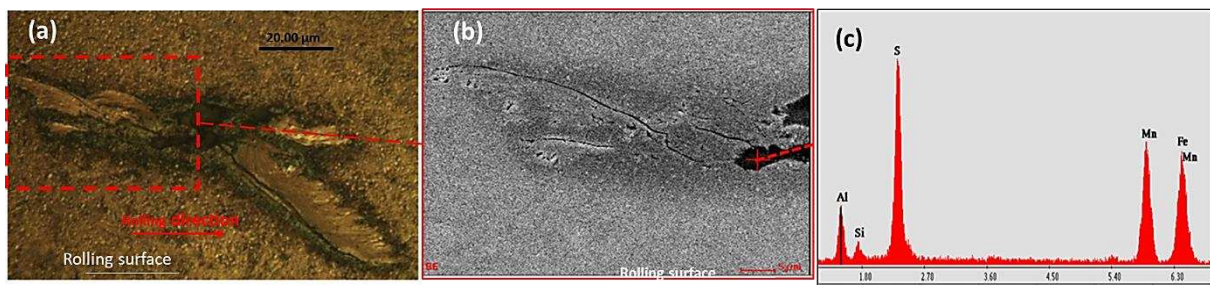


Figure 7. Inclusion initiated the largest butterfly: a) optical image; b) SEM image of one wing; c) EDX of central inclusion.

3.3. Subsurface microcracks

A considerable number of microcracks along a macrocrack are observed on a sample which is over etched as shown in figure 8(a) (marked with white arrows). Further inspections find that considerable microcracks exist on other samples in both axial and circumferential directions as shown in figure 8(b) and 8(c). The considerable number of subsurface microcracks and macrocracks have also been observed in the previous studies [2][22][23][24] however so far limited investigations exist to explain their role on WSF.

Microcracks are found near the sides and ends of the macrocracks where the number of microcracks is much higher than the number of the damaged inclusions. This leads to a postulation that both inclusion and microcracks are the initiators of subsurface microstructural damage leading to WSF. However, the weak boundaries and the residual stress around inclusions play an important role in subsurface damage initiation.

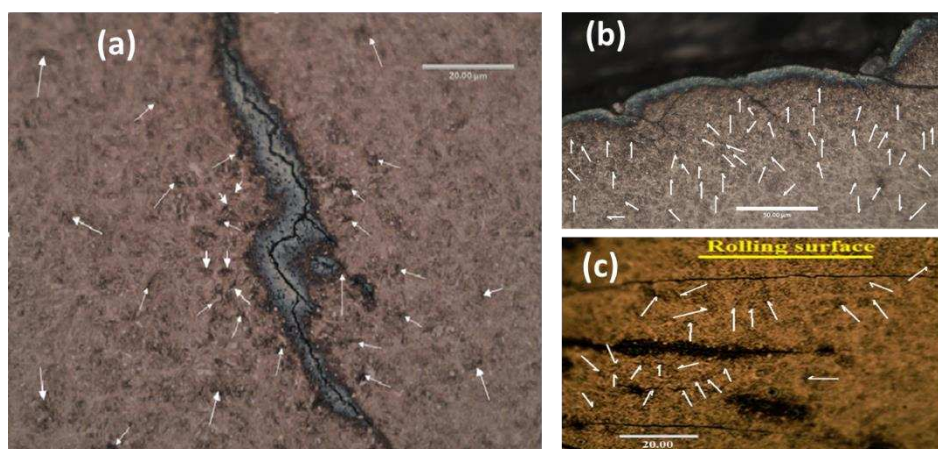


Figure 8. Over etched specimens showing microcracks: a) and b) circumferential sectioned samples c) axial sectioned sample.

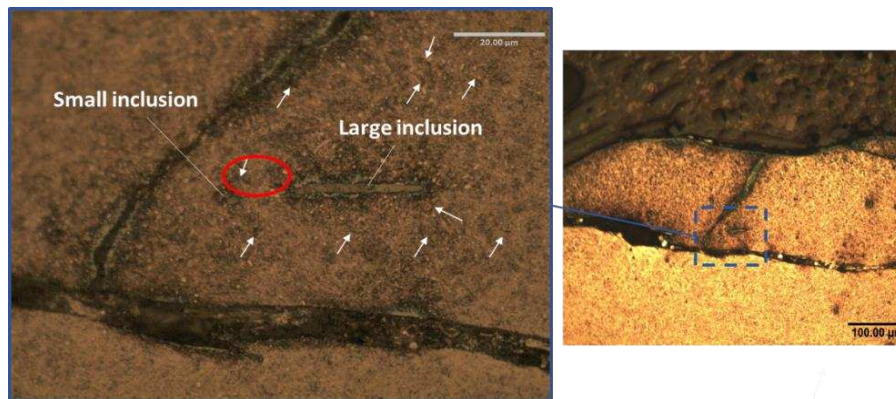


Figure 9. Large inclusion unconnected to surface crack network in axial sectioned sample.

The evidence of the role of subsurface microcracks on damage initiation is also shown in an axial sectioned sample in figure 9. A relatively large inclusion located close to the contact surface does not connect to the macrocracks network around it, despite the inclusion is connected to another small inclusion with a crack (marked with a red ring), the two connected inclusions are not connected to the macrocrack network. A considerable number of microcracks around these two inclusions can be seen (marking by white arrows). This leads to a postulation that subsurface microcracks and/or the cracks initiated from the separation of inclusion boundaries probably propagate towards each other, depending on the direction of the maximum shear stress in high stress locations, they then propagate towards the contact surface causing WSF.

4. Conclusions

This destructive investigation of two failed WTG planetary bearings by microscopic examination has found different forms of damage including butterfly wings, microcracks and damaged inclusions. The following conclusion may be drawn:

- Subsurface microcracks are another damage initiator in addition to non-metallic inclusions to produce subsurface microstructural damage leading to WSF.
- Butterfly wings are associated with the compound type of non-metallic inclusions with low aspect ratios. They are associated with inclusions with internal cracking in a direction approximately parallel to the axis of the maximum wing length.
- Butterfly wings and associated cracks may not be a part of the macrocrack network; the butterflies may firstly have a single wing and the other wing may appear later.
- Characterization of different microstructural damage forms confirms that the maximum shear stress is closely associated with the location of the subsurface microstructural damage.

Acknowledgment:

The authors would like to acknowledge the support of Vestas Wind System A/S by sponsoring this research. The first author would like to thank Iraqi Ministry of Higher Education and Scientific Research (MOHESR) and Engineering College of Misan University, Iraq for sponsoring his PhD study in the University of Sheffield, UK.

References

- [1] M. Evans and M. Evans, "An updated review : white etching cracks (WECs) and axial cracks in wind turbine gearbox bearings," *Mater. Sci. Technology*, vol. **0836**, no. December, 2017.
- [2] J. Lai and K. Stadler, "Investigation on the mechanisms of white etching crack (WEC) formation in rolling contact fatigue and identification of a root cause for bearing premature failure," *wear*, vol.

- 365**, pp. 244–256, 2016.
- [3] S. Sheng; McDade, M.; Errichello, R. Wind turbine gearbox failure modes. In Proceedings of the *International Joint Tribology Conference*, Los Angeles, CA, USA, 24–26 October 2011
- [4] M.-H. Evans, White structure flaking (WSF) in wind turbine gearbox bearings: effects of butterflies and white etching cracks (WECs), *Materials Science and Technology*, vol. **28**, 3–22, 2012.
- [5] Singh, H., et al.: Investigation of microstructural alterations in low- and high-speed intermediate-stage wind turbine gearbox bearings. *Tribol. Lett.* **65** (3), 81, (2017)
- [6] Danielsen, H.K., et al.: Multiscale characterization of White Etching Cracks (WEC) in a 100Cr6 bearing from a thrust bearing test rig. *Wear*, vol. **370**, 73–82 (2017)
- [7] M.-H. Evans, “White structure flaking (WSF) in wind turbine gearbox bearings: effects of ‘butterflies’ and white etching cracks (WECs),” *Mater. Sci. Technol.*, vol. **28**, no. 1, pp. 3–22, 2012.
- [8] S. Mobasher *et al.*, “Effect of non-metallic inclusions on butterfly wing initiation, crack formation, and spall geometry in bearing steels,” *International Journal of Fatigue*, vol. **80**, pp. 203–215, 2015.
- [9] G. Fajdiga and M. Sraml, “Fatigue crack initiation and propagation under cyclic contact loading,” *Eng. Fract. Mech.*, vol. **76**, no. 9, pp. 1320–1335, 2009.
- [10] M. Evans, A. D. Richardson, L. Wang, R. J. K. Wood, and W. B. Anderson, “Confirming subsurface initiation at non-metallic inclusions as one mechanism for white etching crack (WEC) formation,” *Tribology International*, vol. **75**, pp. 87–97, 2014.
- [11] T. Bruce, E. Rounding, H. Long and R. S. Dwyer-Joyce: ‘Characterisation of white etching crack damage in wind turbine gearbox bearings’, *Wear*, **338–339**, 164–177, 2015.
- [12] H. A. AL-Tameemi, H. Long and R. S. Dwyer-Joyce, “Initiation of sub-surface micro-cracks and white etching areas from debonding at non-metallic inclusions in wind turbine gearbox bearing,” *Wear*, vols. **406–407**, pp. 22–32, 2018.
- [13] ISO 4967-2013 — Determination of content of nonmetallic inclusions — Micrographic method using standard diagrams. 2013.
- [14] P. Taylor, B. Jalalahmadi, F. Sadeghi, and V. Bakolas, “Material Inclusion Factors for Lundberg-Palmgren – Based RCF Life Equations Material Inclusion Factors for Lundberg-Palmgren – Based,” *Tribology Transactions*, Vol. **54** (3), pp. 37–41, 2011.
- [15] Y. Murakami and M. Endo, “Effects of defects, inclusions and inhomogeneities on fatigue strength,” *International Journal of Fatigue*, vol. **16**, 1994.
- [16] Y. Murakami, “Material defects as the basis of fatigue design,” *International Journal of Fatigue*, vol. **41**, pp. 2–10, 2012.
- [17] Atkinson HV, Shi G. Characterization of inclusions in clean steels: a review including the statistics of extremes methods. *Prog Mater Sci* 2003; vol. **48**: 457–520
- [18] Lewis MN, Tomkins B. "A fracture mechanics interpretation of rolling bearing fatigue," Proceedings of the Institution of Mechanical Engineers Part J—*Journal of Engineering Tribology* 2012; vol. **226**: 389–485
- [19] Evans M-H, Richardson AD, Wang L, Wood RJK. Serial sectioning investigation of butterfly and white etching crack (WEC) formation in wind turbine gearbox bearings. *Wear* 2013; vol. **302**: 1573–82.
- [20] ISO 281: Rolling bearings — Dynamic load ratings and rating life,” *British Standard*, 2008.
- [21] BS EN 61400-1:2005, Wind turbines Part 1 : Design requirements, *British Standard*, 2010.
- [22] A. Schwedt, L. Wang, W. Holweger, and J. Mayer, “Electron microscopy investigations of microstructural alterations due to classical Rolling Contact Fatigue (RCF) in martensitic AISI 52100 bearing steel,” *International Journal of Fatigue*, vol. **98**, pp. 142–154, 2017.
- [23] N. Shamsaei and A. Fatemi, “Small fatigue crack growth under multiaxial stresses,” *International Journal of Fatigue*, vol. **58**, pp. 126–135, 2014.
- [24] W. H. V Šmeļova, A Schwedt, L Wang, “A study of microstructure alteration in AISI bearings due to classic rolling contact fatigue and white etching crack,” *STLE Annual Meeting & Exhibition*, L. Vegas, USA, 2016.